

Supporting Information for

Bi₂Fe₄O₉ thin films as novel visible-light-active photoanodes for solar water splitting

Yaqiong Wang,^a Matyas Daboczi,^b Camilo A. Mesa,^c Sinclair Ryley Ratnasingham,^{a,d} Ji-Seon Kim,^b James R. Durrant,^c Steve Dunn,^{*e} Haixue Yan,^a and Joe Briscoe^{*a}

^a School of Engineering and Materials Science and Materials Research Institute, Queen Mary University of London, Mile End Road, London E1 4NS, UK. *j.briscoe@qmul.ac.uk

^b Department of Physics and Centre for Plastic Electronics, Imperial College London, South Kensington, London, SW7 2AZ, UK

^c Department of Chemistry, Imperial College London, South Kensington Campus, London SW7 2AZ, UK

^d Department of Materials and Centre for Plastic Electronics, Imperial College London, South Kensington, London, SW7 2AZ, UK

^e School of Engineering, London South Bank University, 103 Borough Road, London, SE1 0AA, UK. *dunns4@lsbu.ac.uk

Experimental Methods

Preparation of Bi₂Fe₄O₉ films

Bi₂Fe₄O₉ thin films were deposited on fluorine doped tin oxide coated float glass (FTO, Tec 15 Pilkington) by CSD method. The glass was cut and cleaned by sonication in acetone and

2-proponal for 15 min each before dried with nitrogen flow. The precursor solution was prepared by dissolving 4 grams of bismuth nitrate ($\geq 98\%$, Sigma-Aldrich, UK) and 6 grams of iron nitrate ($\geq 98\%$, Sigma-Aldrich, UK) in 20 ml 2-methoxyethanol (99.8%, Sigma-Aldrich, UK). 10 ml Acetic anhydride ($\geq 99\%$, Sigma-Aldrich, UK) was then added under constant stirring to the solution to form a homogeneous BFO precursor solution. The precursor with Bi : Fe ratio of 1:2 was prepared for the production of $\text{Bi}_2\text{Fe}_4\text{O}_9$.

$\text{Bi}_2\text{Fe}_4\text{O}_9$ thin films were then prepared by dropping 50 μL of precursor solution onto the substrate and then spin-coating at 3000 rpm for 30 s. As-deposited films were heated in air on a hot plate at 90 $^\circ\text{C}$ for 1 min and then at 350 $^\circ\text{C}$ for 5 min. The films were then transferred into a tube furnace and heated up by 5 $^\circ\text{C}/\text{min}$ to 450 $^\circ\text{C}$ with a dwell time of 30 min before heating to 650 $^\circ\text{C}$ with a ramp rate of 5 $^\circ\text{C}/\text{min}$ and held for 1 hour. The samples were then cooled down within the furnace naturally. All annealing processes were conducted under an oxygen atmosphere. The deposition process was repeated 5 times to achieve a film thickness of around 150 nm.

Characterization

The phase composition of the as-obtained films was analyzed by X-ray diffraction (XRD) using a Panalytical Xpert Pro diffractometer using Cu-K α radiation. The morphology was observed using a scanning electron micro-scope (SEM, FEI Inspect F). X-ray photoelectron spectroscopy was carried out at NEXUS (Newcastle, UK) using a Kratos Analytical AXIS Nova system. Peaks were calibrated to the C1s peak at 284.6 eV. Optical absorption was measured using a Perkin Elmer Lambda 950 UV-Vis spectrophotometer.

The band gap (E_g) of the as-prepared material was calculated using the Tauc relationship¹:

$$(ah\nu)^n = A(h\nu - E_g) \quad (1)$$

where A = constant, $h\nu$ = light energy, E_g = optical band gap energy, a = measured absorption coefficient, $n = 0.5$ for indirect band gap and $n = 2$ for direct band gap materials.

The energy levels and surface photovoltage (SPV) of the $\text{Bi}_2\text{Fe}_4\text{O}_9$ were measured by an APS04 system (KP Technology). The contact potential difference between a 2 mm diameter vibrating gold-alloy tip and the grounded sample was determined and added to the tip's work function to calculate the work function of the sample. A silver reference was used to measure the tip's work function. The contact potential difference was measured in dark until its value saturated and only the final 100 s of the measurement was taken to calculate the Fermi level.

In order to determine the valance band maximum, photoemission was measured while illuminating the sample with monochromatic UV light in the range of 5.4 to 7.0 eV. The cube root of photoemission was plotted and extrapolated to zero to calculate the valance band maximum.

For SPV measurements the work function was monitored in dark for 20 s, then the sample was illuminate by white light (20 mW/cm^2) for 100 s and finally the decay of SPV was measured for an additional 150 s.

Photocatalytic Activity

PEC measurements were conducted in a three-electrode electrochemical system with a potentiostat (Gamry Potentiostat Interface 1000), using a Ag/AgCl reference electrode and Glassy Carbon Rod as the counter electrode. Na_2SO_4 solution was used as the electrolyte (0.2 M, pH 6.5). A solar simulator (Sciencetech, Class: ABA) with an AM 1.5 filter was used for illumination of the system. All PEC measurements were conducted under back illumination in this study.

The measured potential vs. the Ag/AgCl reference electrode was converted into the normal hydrogen electrode (NHE) scale after electrochemical measurements using the Nernst equation:

$$E_{\text{NHE}} = E_{\text{Ag/AgCl}} + E_{\text{Ag/AgCl}}^0 \quad (2)$$

$$E_{\text{Ag/AgCl}}^0 (3.0 \text{ M KCl}) = 0.209 \text{ V at } 25 \text{ }^\circ\text{C} \quad (3)$$

Energetics data

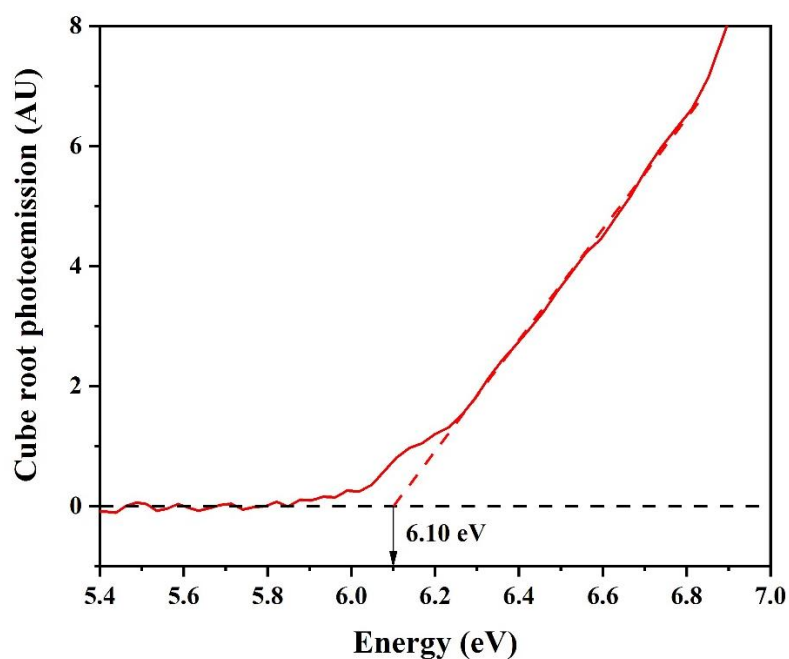


Figure S1. UV-APS data with intercept showing valence band edge of $- 6.10 \pm 0.05$ eV for $\text{Bi}_2\text{Fe}_4\text{O}_9$.

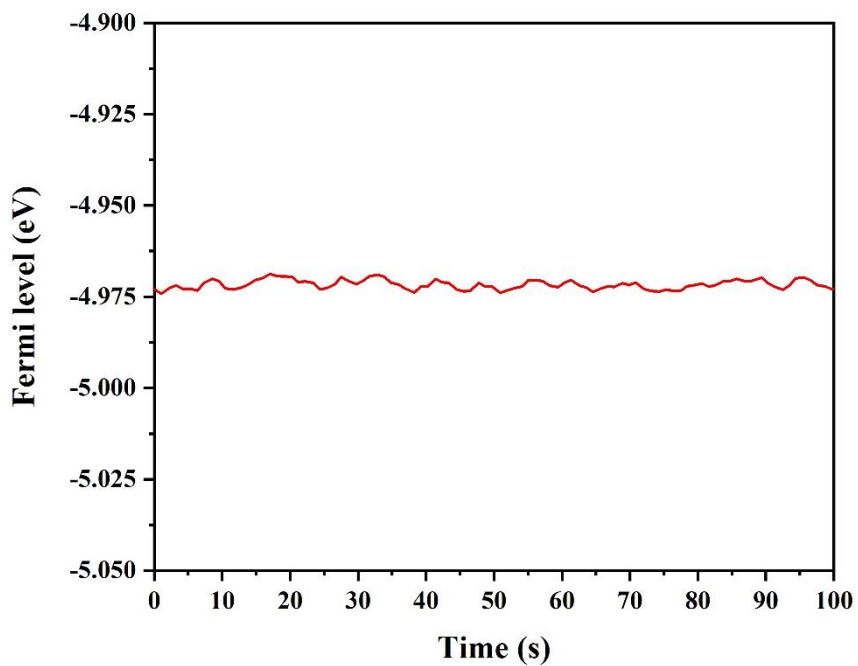


Figure S2. Fermi energy level of $\text{Bi}_2\text{Fe}_4\text{O}_9$ measured by Kelvin probe at -4.972 ± 0.001 eV, showing a very stable value over 100s measured.

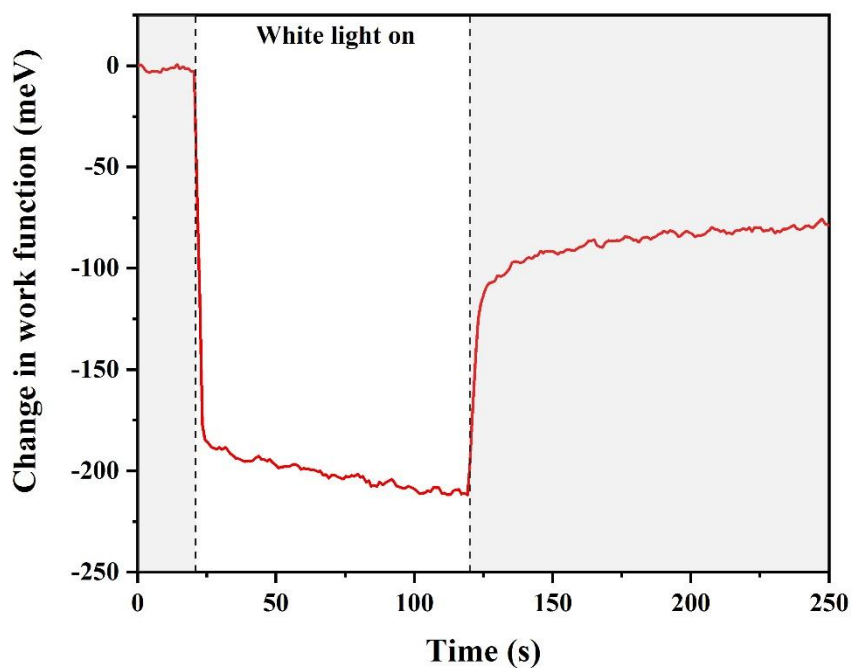


Figure S3. Surface photovoltage measurement showing negative change in work function upon illumination, indicative of an n-type material.

Faradaic efficiency

Oxygen evolution measurements were performed in a gas-tight three electrode cell (electrochemical H-cell, PINE research). A Pt mesh and a Ag/AgCl were used as counter and reference electrodes, respectively. The working electrode ($\text{Bi}_2\text{Fe}_4\text{O}_9$ thin film) was illuminated through the electrode-electrolyte junction using a 365 nm light-emitting diode (LZ1-10U600, LedEngin Inc) with a light intensity of $\sim 20 \text{ mW cm}^{-2}$. The electrolyte used was a 0.2 M Na_2SO_4 solution of Na_2SO_4 .

The Faradaic efficiency was calculated according to equation (4):

$$FE (\%) = \frac{O_{2(\text{measured})}}{O_{2(\text{theoretical})}} \cdot 100 \quad (4)$$

where $O_{2(\text{measured})}$ was measured by a Clark electrode and $O_{2(\text{theoretical})}$ was calculated from the bulk electrolysis (chronoamperometry).

Oxygen was detected using a gas-phase Clark-type oxygen electrode (Unisense OX-NP microsensor) holding the working electrode at 1.2 V vs. Ag/AgCl, where the less recombination and no dark current are observed, as seen in Figure 4a in the main manuscript. The voltage signal sensed by the Clark electrode was converted into mols of oxygen by the calibration curve shown in Figure S4.

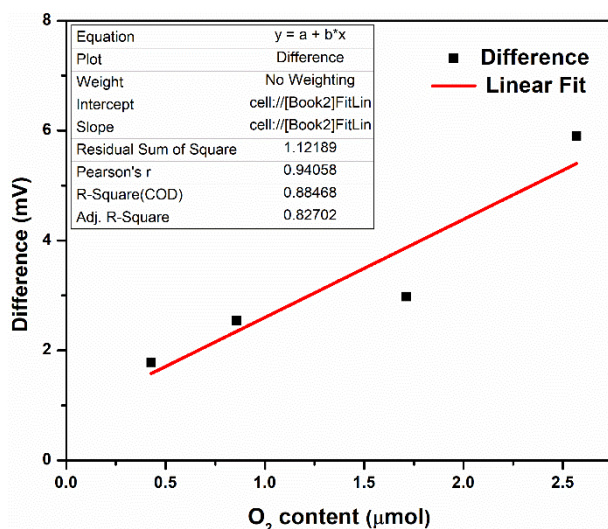


Figure S1. Calibration curve for the Clark electrode injecting known volumes of air as O₂ source.

The theoretical amount of oxygen produced (blue line in Figure S5) during the experiment was calculated from the chronoamperometry (at 1.2 V vs. Ag/AgCl) by integrating the area under the current data (black line in Figure S5), using the following equation:

$$O_{2(\text{theoretical})} = \frac{c}{F \cdot n} \quad (5)$$

where c is the integrated charge (Coulombs), F is the Faraday constant ($96485.3 \text{ C mol}^{-1}$) and n is the number of holes involved in the oxygen evolution reaction (4).

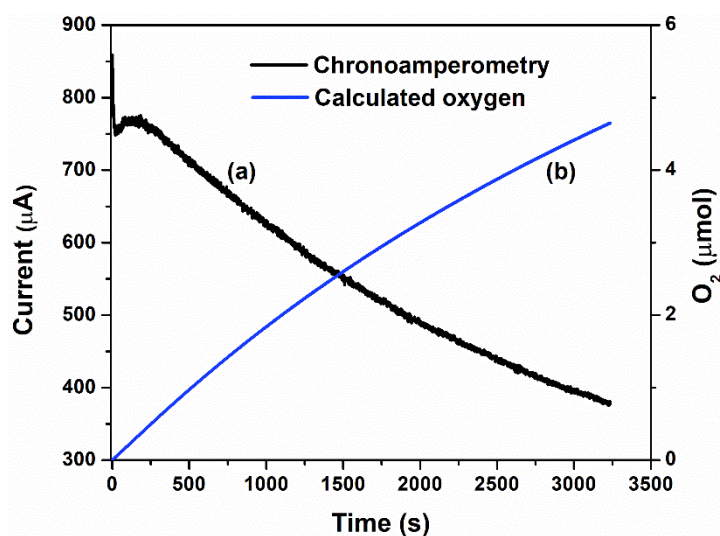


Figure S2. (a) Photocurrent measured as a function of time (chronoamperometry) at 1.2 V vs. Ag/AgCl and (b) amount of oxygen calculated from the chronoamperometric data.

The chronoamperometries and J-V curves performed for the Faradaic efficiency measurements and the ‘Co-Pi’ overlayer deposition were performed using a PGSTAT101 potentiostat (Metrohm Autolab). The J-V curves were performed at 10 mV s^{-1} .

Co-Pi overlayer deposition

A CoO_x overlayer ‘CoPi’ was deposited following the photo-assisted electrodeposition reported elsewhere²⁻⁴. A solution of 0.5 mM of $\text{Co}(\text{NO}_3)_2 \cdot 6\text{H}_2\text{O}$ (99.999%, Sigma-Aldrich) in 0.1 M phosphates buffer (pH 7) was used to perform a photo-assisted electrodeposition under a 365 nm LED, $\sim 20 \text{ mW cm}^{-2}$, illumination conditions and $1.0 \text{ V vs. Ag/AgCl}$ during 300 s , such chronoamperometric data is shown in Figure S6.

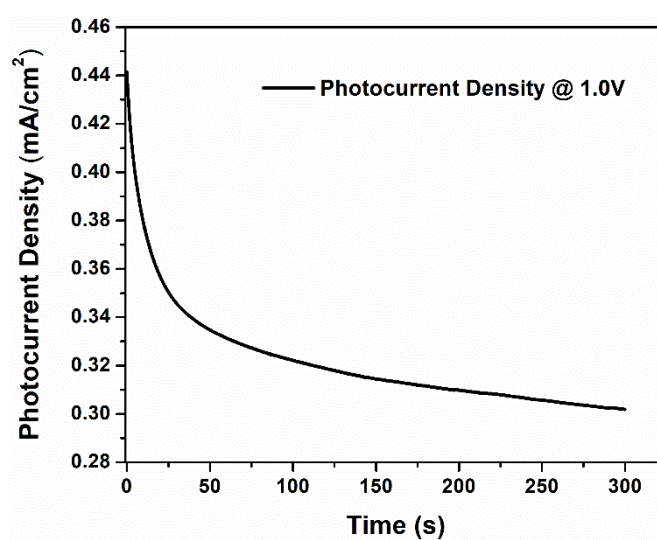


Figure S3. Chronoamperometric data for the photo-assisted electrodeposition of ‘Co-Pi’ overlayer on the $\text{Bi}_2\text{Fe}_4\text{O}_9$ photoanode. The 96.4 C of charged passed correspond to the amount of Co deposited.

Stability in 1 M KOH

In addition to the photostability tests included in the main paper (Figure 4d, inset), stability under illumination (1 sun AM 1.5) and applied potential ($0.23 \text{ V}_{\text{Ag/AgCl}} = 1.23 \text{ V}_{\text{RHE}}$) of the $\text{Bi}_2\text{Fe}_4\text{O}_9$ photoanode was also tested in 1 M KOH (pH 14): Figure S7. This shows an initial

slight increase in photocurrent followed by stabilisation to the original value, indicating good photostability under standard operating conditions.

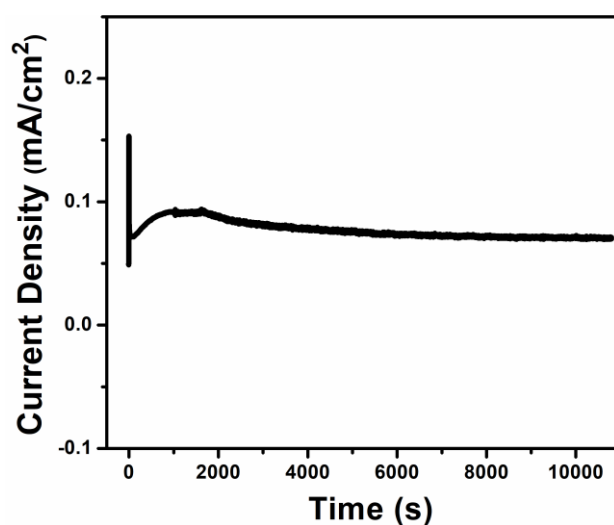


Figure S7. Chronoamperometric data of the Bi₂Fe₄O₉ photoanode tested in 1 M KOH at 0.23 V_{Ag/AgCl} = 1.23 V_{RHE} under 1 sun AM 1.5 illumination (switched on at $t = 0$).

- 1 Tauc, J., Grigorovici, R. & Vancu, A. Optical properties and electronic structure of amorphous germanium. *physica status solidi (b)* **15**, 627-637 (1966).
- 2 Barroso, M. *et al.* Dynamics of photogenerated holes in surface modified α -Fe₂O₃ photoanodes for solar water splitting. *Proceedings of the National Academy of Sciences* **109**, 15640-15645 (2012).
- 3 Zhong, D. K., Cornuz, M., Sivula, K., Grätzel, M. & Gamelin, D. R. Photo-assisted electrodeposition of cobalt-phosphate (Co-Pi) catalyst on hematite photoanodes for solar water oxidation. *Energy & Environmental Science* **4**, 1759-1764 (2011).
- 4 Kanan, M. W. & Nocera, D. G. In situ formation of an oxygen-evolving catalyst in neutral water containing phosphate and Co²⁺. *Science* **321**, 1072-1075 (2008).